Atomic Energy of Canada Limited

GENTILLY BLW BOOSTER ROD EXPERIMENTS IN THE ZED-2 REACTOR

by

M.H.M. ROSHD

Chalk River, Ontario

February 1969

AECL-3258

GENTILLY BLW BOOSTER ROD EXPERIMENTS IN THE ZED-2 REACTOR

by

M.H.M. Roshd

A B S T R A C T

Measurements were performed in ZED-2 on simulated BLW 61-element boosters containing 5, 6.56 and 7.46 g of U^{235} per cm length. These boosters either replaced the central fuel assembly in a rod centred lattice or were located interstitially in an open centre lattice.

The boosters' perturbing effects on the neutron density distribution and the epithermal index $r\sqrt{T_n/T_o}$ were investigated. The fine structure and the reactivity worth of each booster were measured in the two lattices. The reactivity of the 5 g/cm booster was also measured as a function of radial position.

Reactor Physics Branch
Chalk River Nuclear Laboratories
February 1969

AECL-3258

CONTENTS

TABLES

FIGURES

FIGURES (cont'd)

GENTILLY BLW BOOSTER ROD EXPERIMENTS IN THE ZED-2 REACTOR

1. INTRODUCTION

This report describes a series of measurements performed in the ZED-2 reactor to investigate the neutronic effects of the proposed Gentilly BLW booster rod.

To start the BLW reactor in a reasonably short time after a shut-down, an excess reactivity of about 35 milli-k must be provided to compensate for the build-up of the Xe-135 poison and to overcome the effect of the increase in the coolant density due to water replacing steam in the coolant channels. For this purpose booster rods containing a high concentration of U^{235} are introduced interstitially and perpendicular to the fuel assemblies. However the introduction of these booster rods in a reactor lattice results in strong flux perturbations with peaks in the vicinity of the boosters. The aim of this series of measurements was to investigate these perturbations as well as the reactivity worths of the booster rods and the neutron density fine structures associated with them.

A previous design of BLW booster was studied by Kay[1] but initial analysis of these measurements using EQUIPOISE and POOOF/KEFF programs[2] resulted in a large discrepancy between experiment and theory.

A later MICRETE-LATREP[3] analysis resolved the discrepancy, and good agreement was obtained. The analysis of Kay's experiments, however, was made more difficult by the rectangular geometry of the booster cluster and the complicated nature of the core. To mock up BLW, the fuel assemblies were H_2O cooled and a large driver-buffer region was necessary to achieve criticality. It was felt that greater confidence in the calculational method would result from analysis of experiments in "clean", undriven, air cooled lattices using cylindrical boosters with different U-235 concentrations.

2. EXPERIMENTAL ARRANGEMENTS

2.1 The Lattices:

The BLW lattice was simulated in the heavy water moderated ZED-2 reactor using the 28-element natural UO_2 fuel assemblies

shown in Fig. 1 in a square lattice of 27.94 cm pitch. All the assemblies were air-cooled. Two lattice configurations were used: (a) an open centre lattice as shown in Fig. 8 and 10 at whose centre the booster was located interstitially in a vertical position, (b) a rod-centred lattice in which the booster replaced the central fuel assembly (Fig.9 and 11).

The booster rod was also placed at different radial positions in these lattices as will be described later.

2.2 The Booster Rods and their Suspension System:

The boosters consisted of 61 fuel elements arranged in five rings as shown in Fig. 2. The clusters were assembled with two drilled end plates and four spacer plates. Individual elements could easily be withdrawn axially. Each element, 216.2 cm long, consisted of a core of uranium-aluminium alloy 0.386 cm diameter, (the uranium was 93.16% enriched) sheathed in aluminium (0.772 cm OD). The cores and sheaths were not separable (Fig. 3).

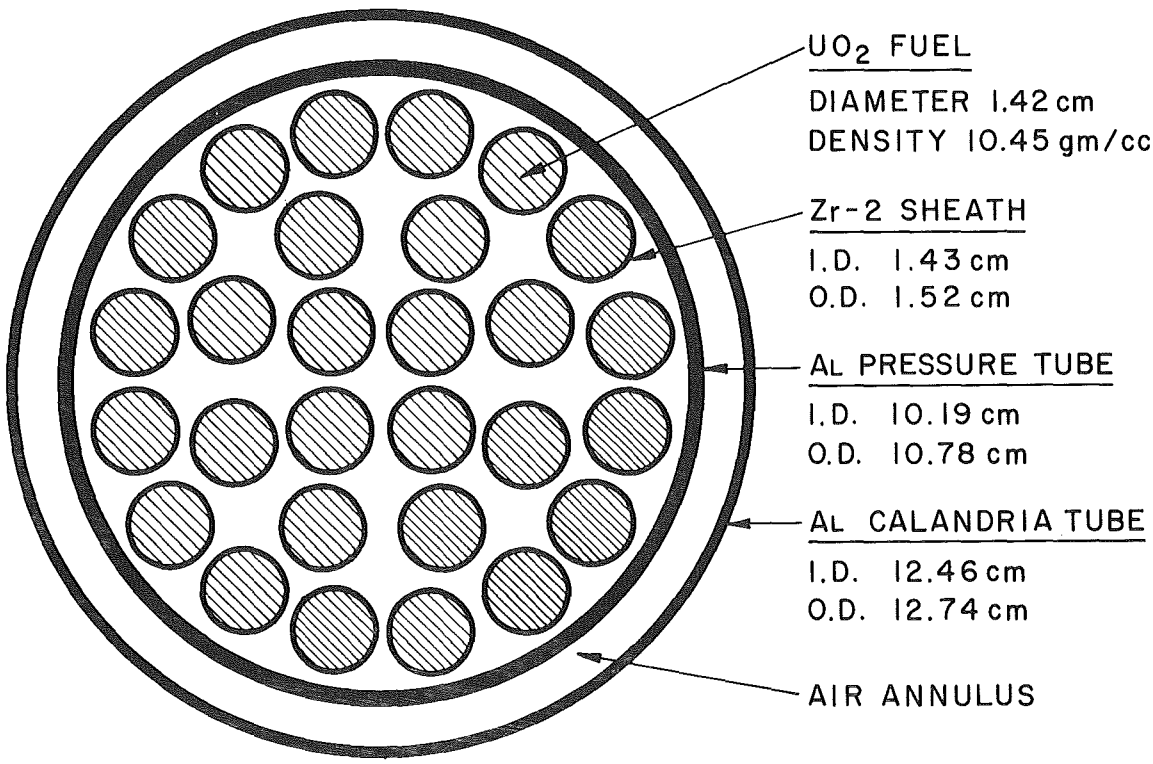

Fig. 1. Cross section of 28-element natural UO_2 assembly

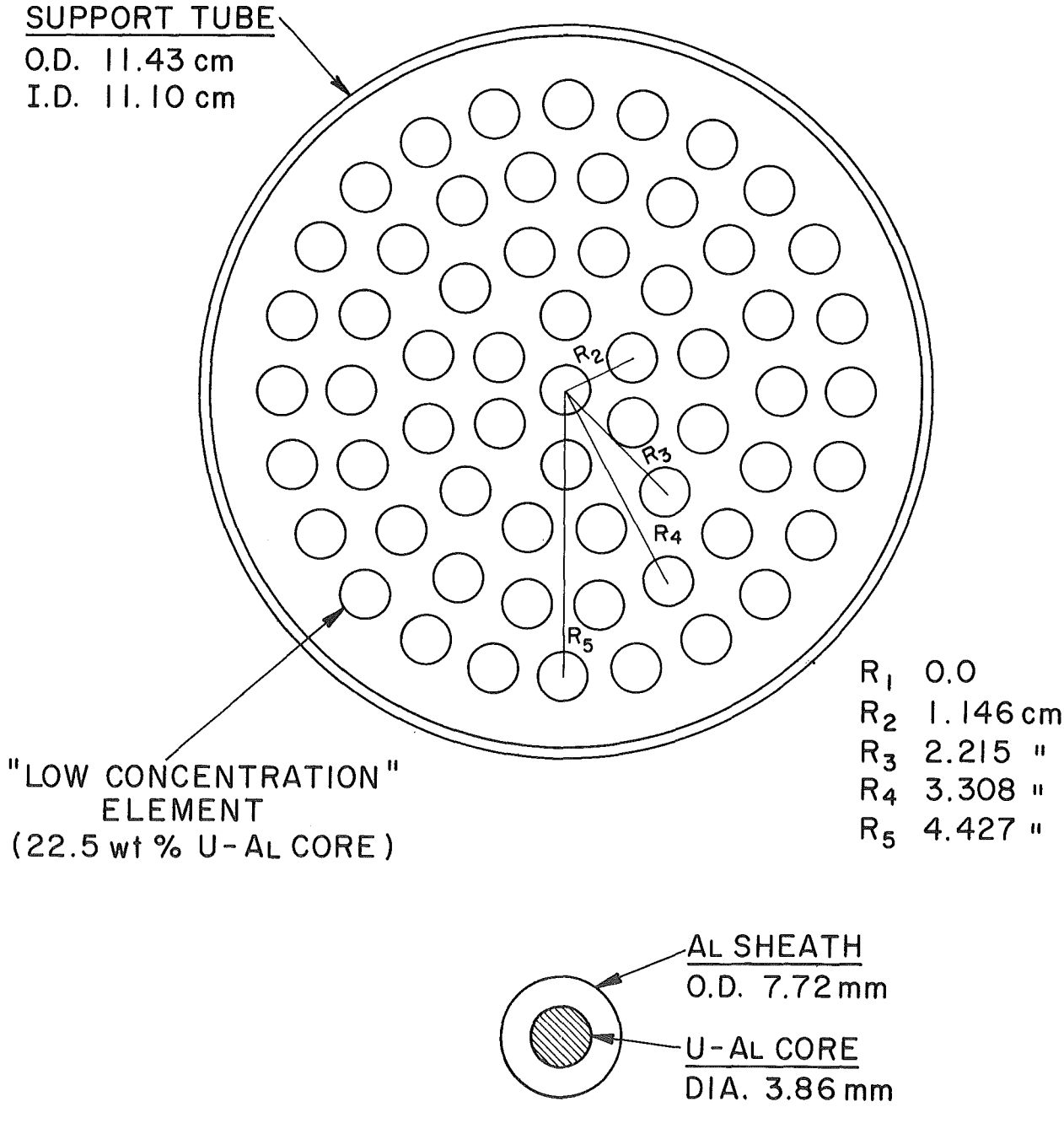

Fig. 2. Gentilly booster BI (5g U^{235}/cm)

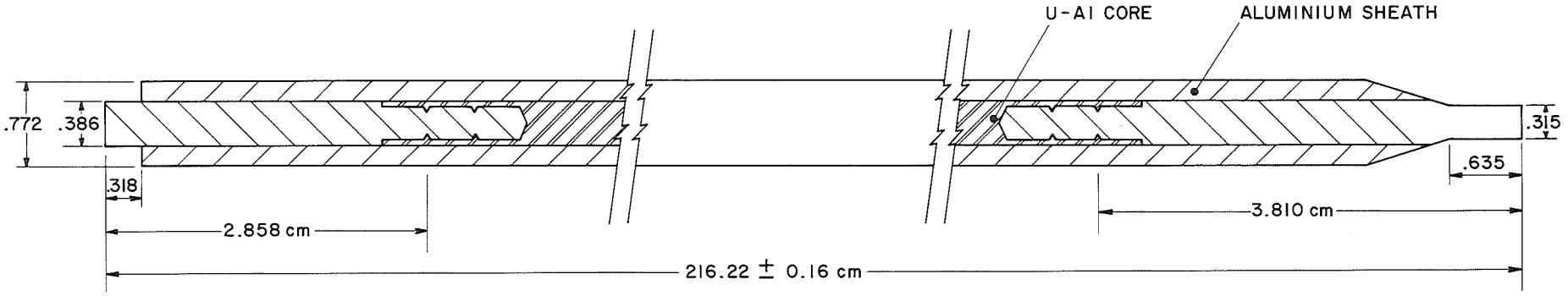

Fig. 3. Booster normal fuel element

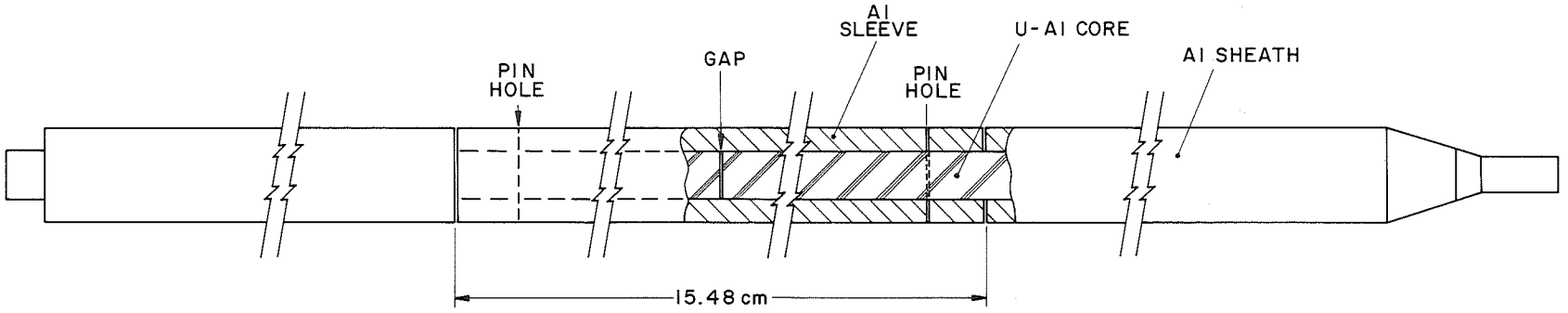

Fig. 4. Demountable element

The U-Al alloy was available with two concentrations, namely a "high concentration" of 37.7 wt % uranium and a "low concentration" of 22.5 wt % uranium. More than 61 elements of the latter type and 34 of the former type were available.

Three boosters were assembled. One consisted of low concentration elements only (Booster BI) and had a U^{235} density of 5 g[(a)] per cm length. The other two were mixtures of the two types of elements in the same cluster. Booster BII was a two-zone arrangement with 42 of the low concentration elements in the two outer rings and 19 high concentration elements occupying the central region of the cluster as shown in Fig. 5. The loading of this booster was 6.56 g[(a)] U^{235} per cm. Booster BIII consisted of 31 low concentration elements and 30 high concentration elements uniformly distributed as shown in Fig.6. The U^{235} loading was 7.46 g/cm[(a)].

Eight elements of each type were demountable and each element consisted of two sections of equal length. One end of each section had 7.7 cm of its Al sheathing removed and the bare ends were butted together inside a sleeve (of the same dimensions as the removed sheathing) and secured with pins (Fig. 4). With this arrangement it was hoped that measurements could be taken of the average neutron density in the fuel core by putting foils between the two bare ends.

During the measurements the booster cluster was housed in an aluminium tube 231.1 cm long, with an outside diameter of 11.43 cm and a wall 1.65 mm thick. The top flange[(4)] of this tube was bolted to the flange of a second Al tube 166 cm long and the lower end was extended with a tube section 10.63 cm long. This booster assembly was suspended from an Al suspension bar bolted to the top of two Al clamps, which were in turn firmly attached to the two central lattice beams (Fig. 7). The bottom of the assembly was 3 mm only from the reactor vessel floor to avoid any reactivity increase due to the booster falling to the floor. A safety bracket was welded to the top of the booster assembly and was fitted around the two support clamps. This arrangement ensured that the booster would not tip over into the reactor if the suspension system were to fail. Critical height measurements indicated that the positioning of the booster was reproducible with good accuracy.

(a) These are nominal U^{235} densities and are used throughout the report. The actual U^{235} loadings are 4.88, 6.35 and 7.20 g/cm corresponding respectively, to the nominal loadings of 5.00, 6.56 and 7.46 g/cm.

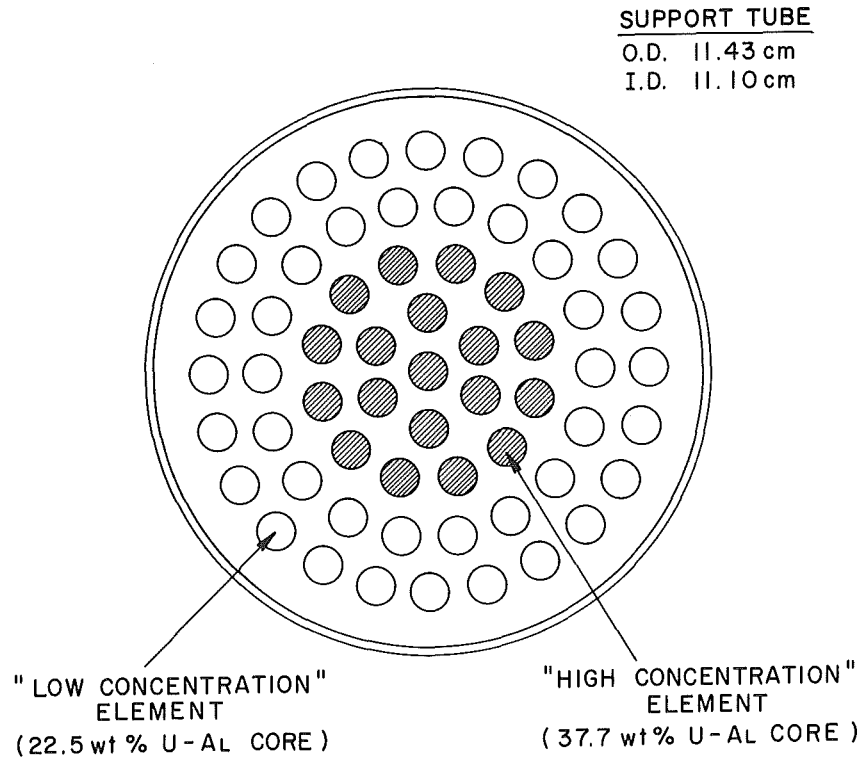

Fig. 5. Gentilly booster BII (6.56 g U^{235}/cm)

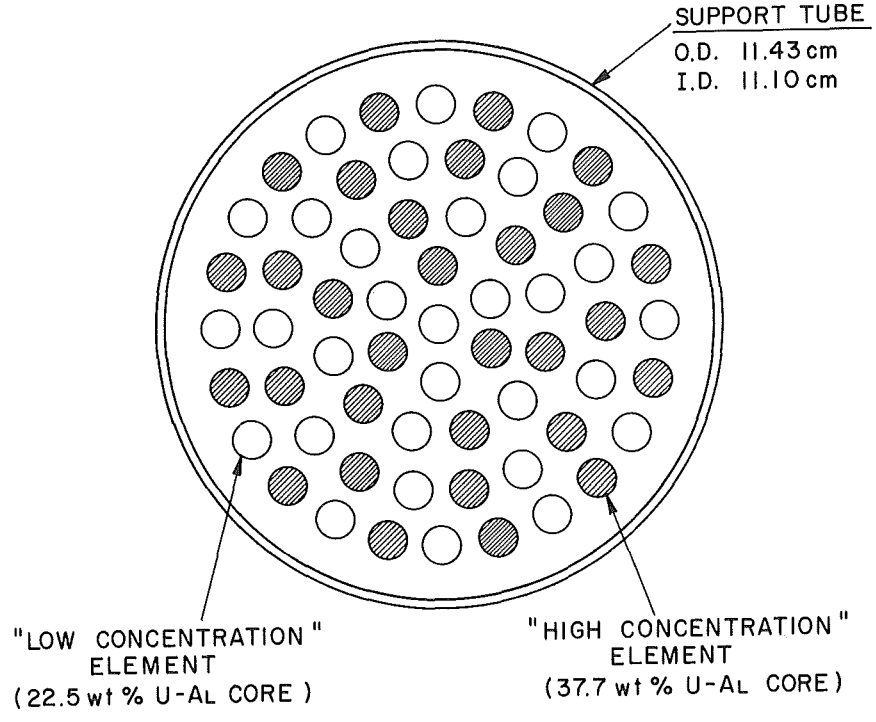

Fig. 6. Gentilly booster BIII (7.46 g U^{235}/cm)

The level of D_2O in the booster support tube was the same as that of the D_2O moderator in the ZED-2 reactor.

3. EXPERIMENTAL PROCEDURES

3.1 Neutron Density Measurements:

To determine the perturbation effects due to each booster rod the neutron density was determined by foil measurements in the reference lattices (i.e. without a booster rod) and in the perturbed lattices (i.e. when a booster rod was introduced).

Fig. 8 and 9 show the foil loadings in the reference lattices. At cell boundary positions, thin walled Al thimbles contained 1.13 cm diameter, 0.025 cm thick Cu foils. In the open centre lattice thimbles F9, F6, F0 and G0 held full sets of foils at 10 cm intervals from an elevation of 15 cm to 205 cm. The rest of the thimbles carried Cu foils at elevations of 90 and 120 cm (the elevations were measured from the reactor vessel floor). Similar Cu foils were taped on the calandria tubes of the fuel assemblies F1, F3, F5 and F7 in the north, west, south and east directions at elevations of 90 and 120 cm. A full set of foils was also used on the north side of F1.

The foil loading in the rod centred reference lattice was as shown in Fig. 9.

Measurements in the perturbed lattices were done in the same manner. The Cu foils were located in the same positions as in the reference lattices (Fig. 10 and 11). In addition, foils were taped on the booster support tube at elevations of 90 and 120 cm.

The fine structure in each booster cluster was also determined using Cu detectors. The average neutron density in the fuel was measured by placing Cu foils (3.86 mm diameter and .13 mm thick) between the tips of the unsheathed parts of the demountable elements at an elevation of 120.1 cm. The Cu foils were sandwiched between 0.025 mm thick Al foils of the same diameter to stop contamination by fission fragments. In order to measure the average neutron density on the surface of the booster elements, Cu strips .13 mm thick and 5 mm wide were taped around the demountable elements at elevations of 105.1 and 116.3 cm. The demountable elements were distributed in the cluster in such a way as to avoid any interference between the foils.

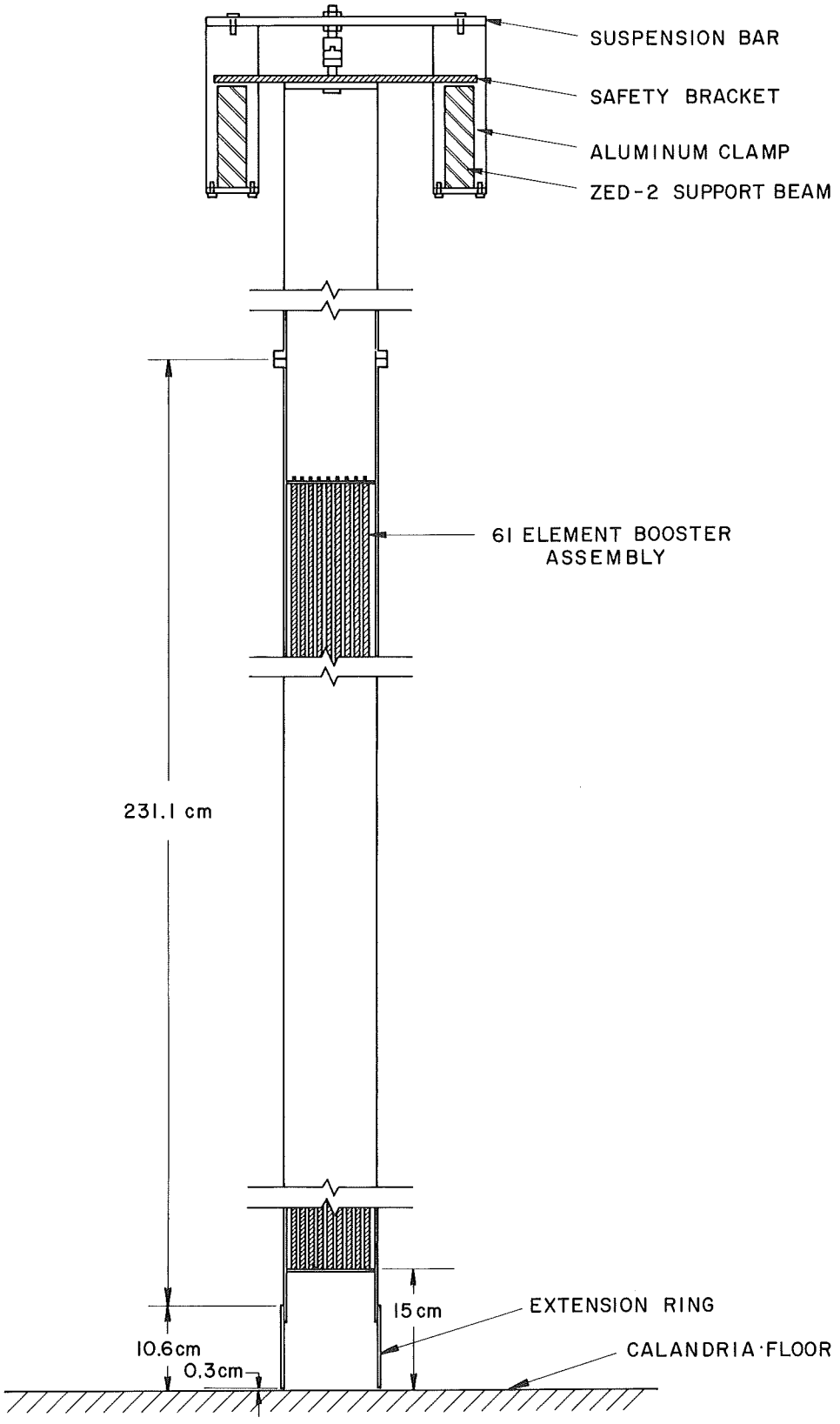

Fig. 7. Booster rod suspension system

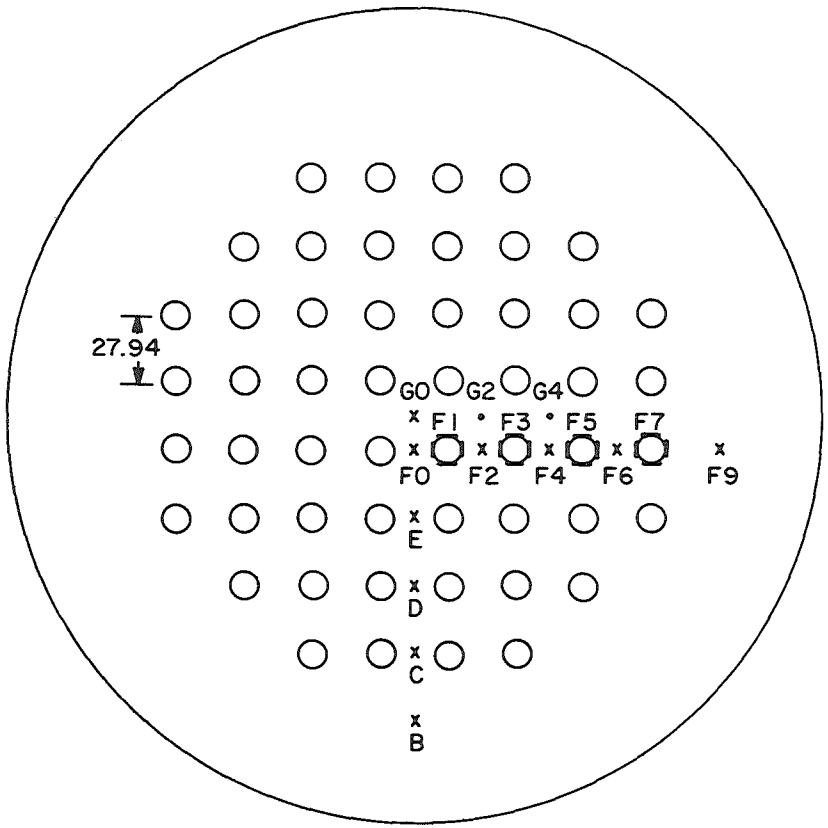

Fig. 8. Open centre reference lattice - Foil loading

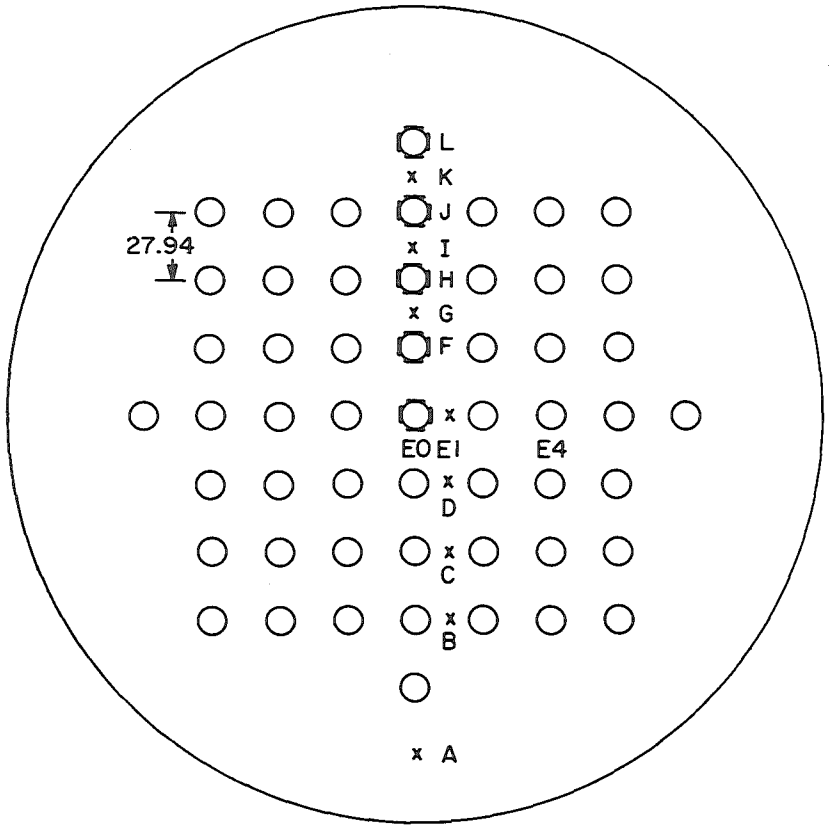

Fig. 9. Rod-Centred reference lattice - Foil loading

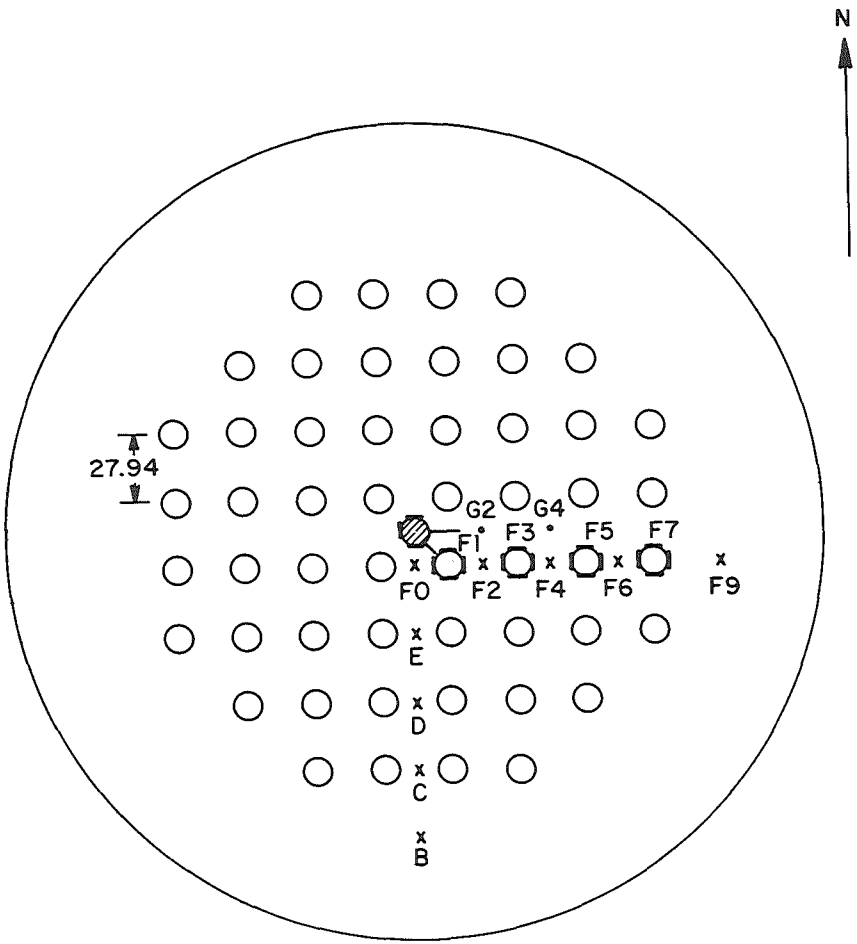

Fig. 10. Open Centre lattice & booster - Foil loading

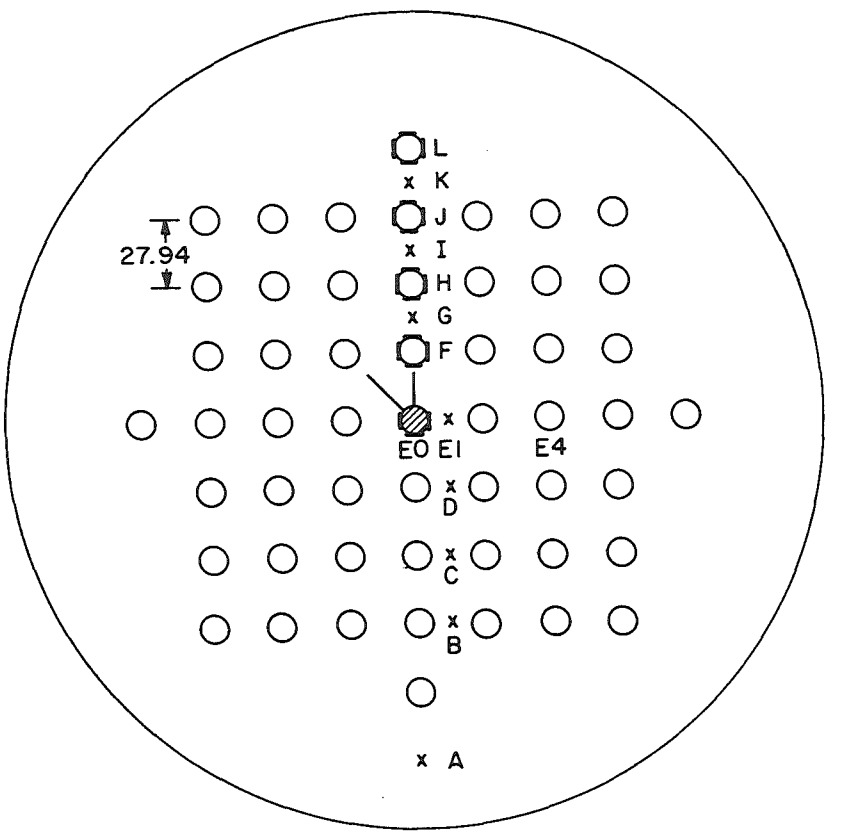

Fig. 11. Rod-Centred lattice & booster - Foil loading

The neutron density distribution in the moderator surrounding the booster tubes was measured with 1.13 cm diameter 0.025 cm thick Cu foils mounted at 2 cm intervals on thin Al strips taped to the booster tube in the directions shown in Fig. 10 and 11.

3.2 $r\sqrt{T_n/T_o}$ Measurements:

The neutron spectrum perturbations can be inferred from measurements of $r\sqrt{T_n/T_o}$ at several points in each of the lattices used. This index was determined for the unperturbed lattices by measuring the activity ratios of pairs of In and Cu foils. These ratios were normalized to the activity ratio of a similar pair located in a reference position (F9 in the case of the open centre lattice and FO for the rod centred lattice) where the $r\sqrt{T_n/T_o}$ value was determined from the In-Cd ratio. The Cu foils were the same as those used for macroscopic flux measurements and the In foils (1% In-Al alloy) were 1.13 cm diameter, 0.025 cm thick. These foil pairs were located at an elevation of 120 cm.

For measurements with a booster in the ZED-2 core it was not possible to use In foils because of their short half life and due to the high radiation from the booster several hours after an experiment. Gold foils (1.13 cm diameter, 0.025 mm thick) were used instead and thus it was possible to wait overnight before unloading the foils.

$r\sqrt{T_n/T_o}$ values in the booster cluster were obtained from Au strips 0.025 mm thick and 5 mm wide taped around the sheaths of three demountable elements on top of Cu strips at an elevation of 116.3 cm.

The activity ratios of Au and Cu foils were normalized to that of a similar pair in the reference position where the $r\sqrt{T_n/T_o}$ was assumed to be the same as in the unperturbed lattice measurements.

3.3 Critical Height Measurements:

The reactivity worth of each booster was determined by measuring the critical height of the unperturbed reference core and the core with the booster. The changes in the moderator height were determined with an accuracy of ±0.03 mm.

In the open centre lattice the following critical height measurements were taken:

(a) bare pile,

(b) each booster rod (i.e. the cluster + the suspension system) suspended vertically at the centre of the lattice,

(c) the suspension system only at the centre of lattice,

(d) the booster rod BI placed at the off-centre positions : G2E and G4E,

(e) the suspension system only at the off-centre positions G2E and G4E,

(f) a full length 2.54 mm diameter cobalt wire located at the centre of the lattice.

For the rod-centred lattice the measurements (a), (b) and (c) were repeated. In addition critical heights were measured with:

(g) the booster rod BI in the off-centre position E4E,

(h) the Co wire at the edge of the central cell, i.e. at E1E.

The measurements with the Co wire were used to convert the changes in critical height to changes in reactivity.

4. RESULTS AND DISCUSSIONS

4.1 Perturbation Effects of the Boosters:

The radial and axial flux distributions were measured at different locations in the two lattices with and without the boosters. The complete results are given in Appendix I. The data were normalized to 1.000 at the position F9 (Z=90) for the open centre lattice and at the position F0 (Z=90) for the rod-centred lattice.

Considering the various sources of possible errors - statistical, positional, sensitivity of detectors, etc. - the uncertainty in data was estimated to be less than 1.5%.

The measured values of $r\sqrt{T_n/T_o}$ given in Table 1 were used in the familiar expression:

$$n(r,z) \alpha \frac{A(r,z)}{G_{th}g + G_r S_o \, r\sqrt{T_n/T_o}}$$

to obtain the neutron densities n(r,z) from the measured activities A(r,z). The various parameters in the expression are well known. At points where no measurements were taken, $r\sqrt{T_n/T_o}$ was assumed to be inversely proportional to foil activities.

The strong perturbation effects due to the introduction of boosters at the centre of a lattice are illustrated in Figures 12a, b. However these effects are best described in terms of a flux perturbation factor F(r,Z) defined as

$$F(r,Z) = \frac{\frac{n(r,z)}{n(R,Z)}\ \text{perturbed}}{\frac{n(r,z)}{n(R,z)}\ \text{unperturbed}}$$

Table 1. Measured $r\sqrt{T_n/T_o}$ values

(1) Open-Centre Lattice

Location	F9	F4	F3-W[a]	F2	E0	F1-W	F0	Booster G0-W	Booster R5	Booster R3	Booster R2	Booster R1
Reference lattice	.0048	.028	—	.029	.028	—	.028					
Lattice + BI	.0048	.030	(.061)	.032	.031	(.090)	.048	—	.080	.105	—	.116
Lattice + BII	.0048	.031	—	.031	—	.055	.047	.080	.086	.122[b]	—	—
Lattice + BIII	.0048	—	—	.032	—	.050	.048	.081	—	—	.135[b]	—

( ): these values are suspiciously high and should be rejected

(2) Rod-Centred Lattice

Location	A	J-S	I	H-S	G	F-S	E1	Booster E0-S	Booster R5	Booster R3	Booster R2	Booster R1
Reference lattice	.0044	—	.030	—	.029	—	—					
Lattice + BI	.0044	—	.033	.038	.032	.038	.034	.053	.056	.074	.075	—
Lattice + BII	.0044	.035	.031	—	.030	.035	.036	—	.055	.081[b]	—	.093[b]
Lattice + BIII	.0044	.034	—	—	—	.036	.035	—	.066	.090	.090	—

(a) West side of calandria tube

(b) measured at the sheath surface of "high concentration" elements.

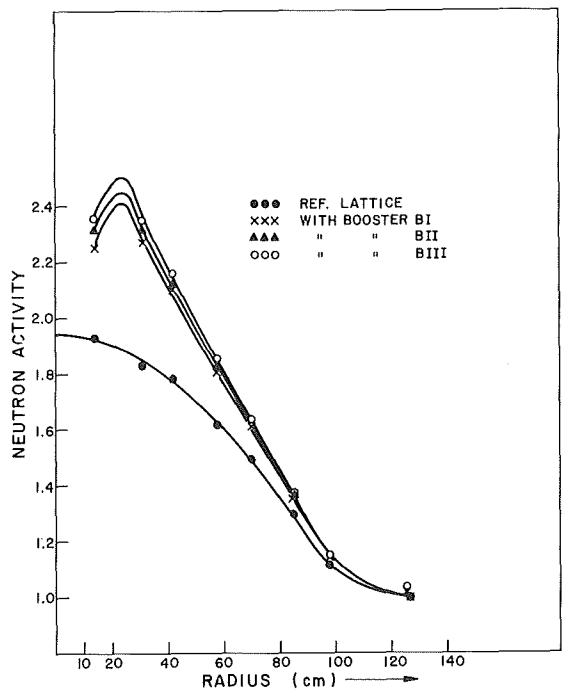

Fig. 12a. Radial activity distributions in open centre lattice with boosters

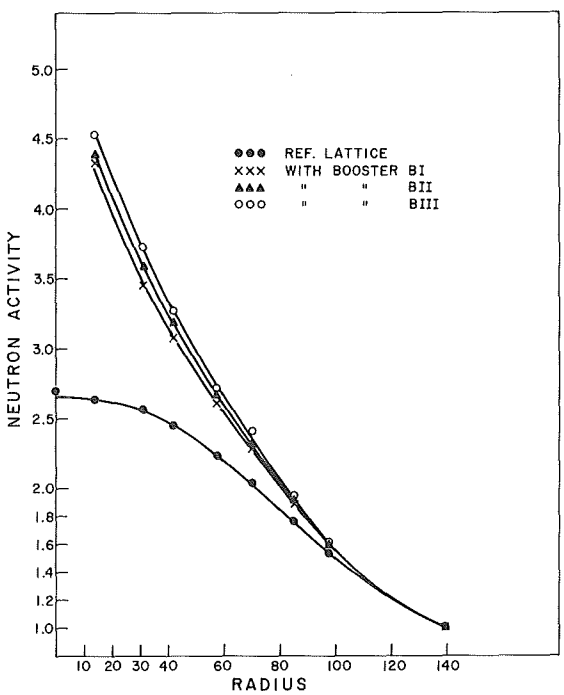

Fig. 12b. Radial activity distributions in rod-centred lattice with boosters

Table 2. Flux perturbation factor F(r,z) - open centre lattice

Position	Radius (cm)	with booster BI		with booster BII	with booster BIII
		F(r,120)	F(r,90)	F(r,120)	F(r,120)
F9	126.51	1.0017	1.0069	1.0071	1.0039
B	125.73	0.9983	0.9931	0.9930	0.9960
F7	98.78	1.0303	1.0333	1.0290	1.0344
C	97.79	1.0393	1.0330	1.0339	1.0399
F6	84.98	1.0602	1.0516	1.0542	(1.0251)
F5	71.23	1.0796	1.0827	1.0833	1.0986
D	69.85	1.0890	1.0865	1.0817	1.1042
F4	57.60	1.1216	1.1246	1.1204	1.1549
F3	44.18	1.1752	1.1666	1.1838	1.2095
E	41.91	1.1781	1.1901	1.2072	1.2359
F2	31.24	1.2426	1.2515	1.2520	1.2753
G2W	27.94	1.2698	—	—	—
F1	19.76	1.2225	1.2250	1.2495	1.2757
F0	13.97	1.1742	1.1798	1.1876	1.2047

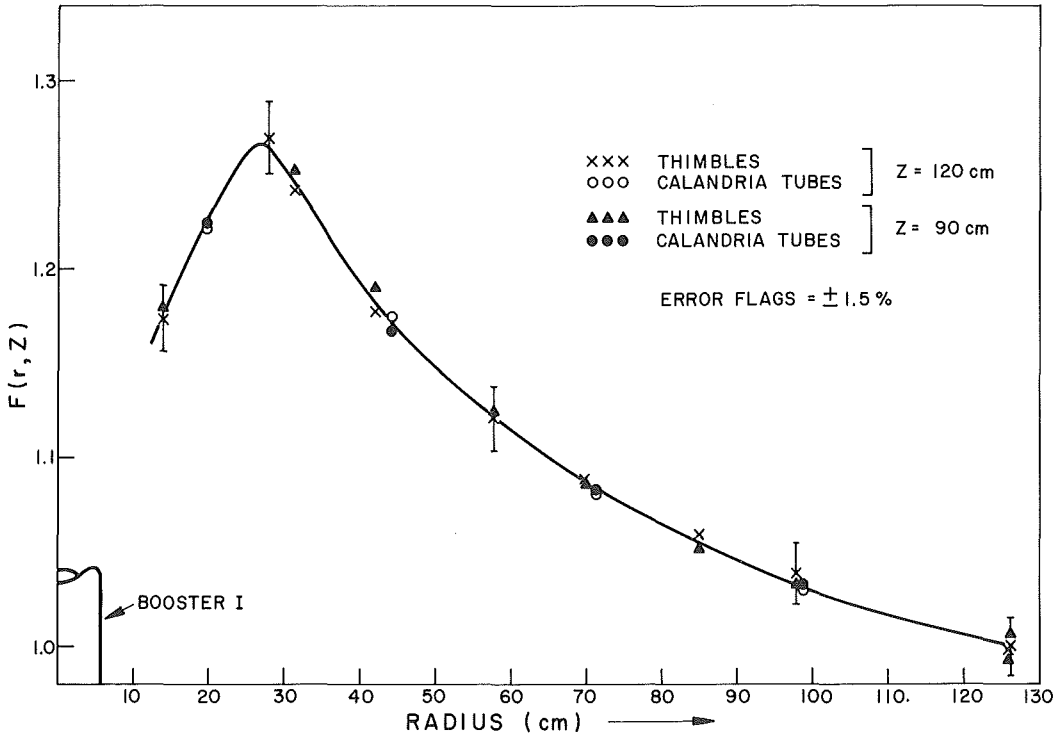

Fig. 13. Flux perturbation factor - open centre lattice with booster BI

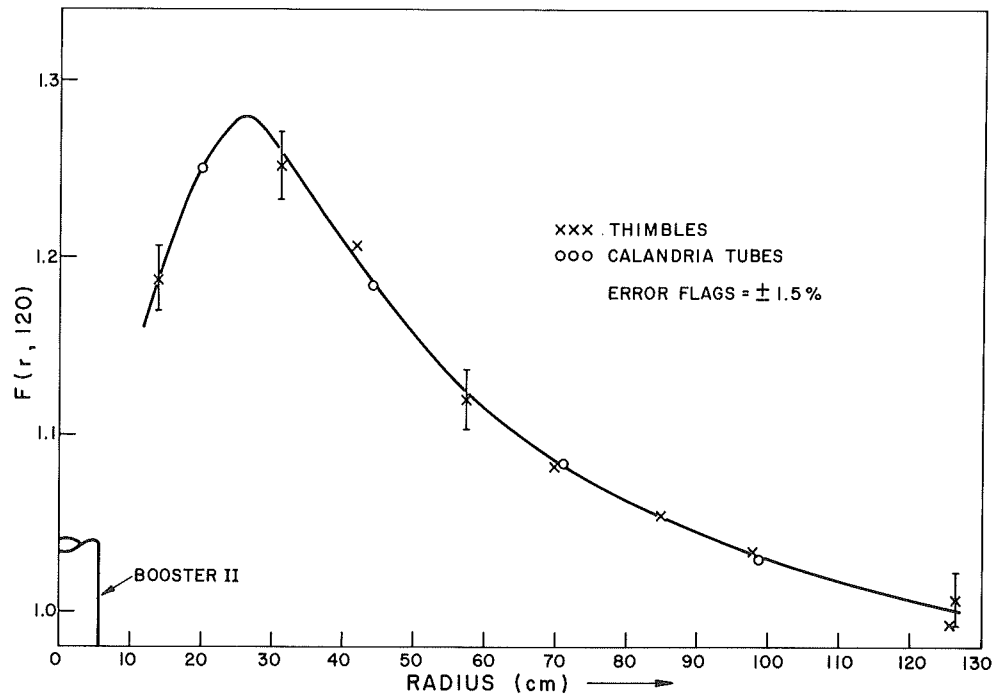

Fig. 14. Flux perturbation factor - open centre lattice with booster II

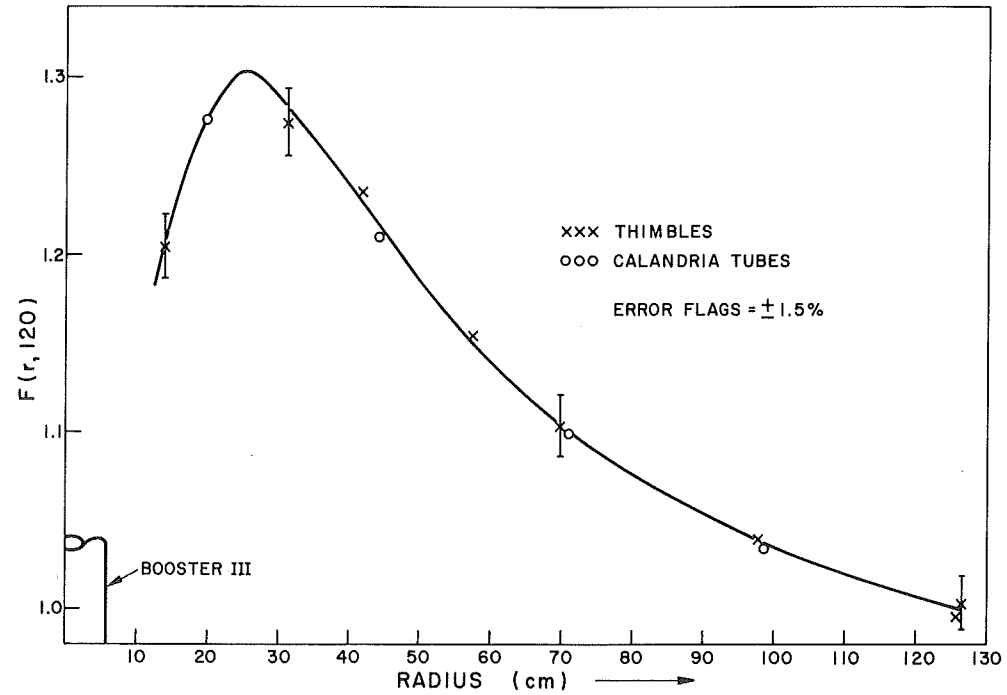

Fig. 15. Flux perturbation factor - open centre lattice with booster BIII

where R refers to a point outside the perturbed region. The flux perturbation factors in the open centre lattice for the three boosters are given in Table 2 and shown in Fig. 13, 14 and 15. It must be recalled here that measurements at the surface of each calandria tube were taken in four directions, however only the average values were plotted at radii corresponding to the distances of the centres of the calandria tubes from the centre of the ZED-2 core.

It can be seen that a booster, acting as a strong source of fast neutrons, produces a general increase in the neutron density. At the same time a booster behaves as a strong thermal neutron absorber (due to the high concentration of U^{235}) producing a depression of neutron density in its immediate neighbourhood. Thus F(r,z) peaks at ~26 cm from the centre of the booster.

Looking more closely at Table 2 and Fig. 13 - 15 it is found that the average values of F(r,z) at the calandria tubes of the neighbouring 28-element fuel assemblies for the 5, 6.56 and 7.46 g/cm boosters are 1.223, 1.250 and 1.276 respectively. It is evident, therefore, that the increase in neutron density is not proportional to the U^{235} concentration, due to self shielding in these heavily loaded boosters.

The perturbation effects of the boosters in the rod-centred lattice are given in Table 3 and Fig. 16 - 18. The F(r,z) peaks observed in the previous case must now be much closer (~10 cm) to the booster rods. However the nearest measurement point in the reference lattice was at the edge of the central cell, at r = 13.97 cm, and therefore these peaks could not be shown in the figures.

Comparison between the two sets of results, those of the open centre lattice and those of the rod centred lattice, shows that the general increase in neutron density due to the same booster rod is lower for the former due to the larger mutual shielding resulting from higher fuel to moderator ratio in the central region of the core. This also results in a harder spectrum in this region (compare the measured values of $r\sqrt{T_n/T_o}$ in Table 1).

Table 3. Flux perturbation factor F(r,z) - Rod-centred lattice

Position	Radius(cm)	with booster BI F(r,120)
A	139.70	1.0000
L-N	118.13	1.0346
S	105.39	1.0297
E	111.94	1.0157
W	111.94	1.0383
K	97.79	1.0507
J-N	90.19	1.0701
S	77.45	1.0893
E	84.06	1.0980
W	84.06	1.0497
I	69.85	1.1096
H-N	62.25	1.1630
S	49.51	1.2152
E	56.23	1.1881
W	56.23	1.2035
G	41.91	1.2591
F-N	34.31	1.3489
S	21.57	1.4688
E	28.65	1.4114
W	28.65	1.4079
E1	13.97	1.5986
D	31.24	1.3842
C	57.59	1.1931
B	84.98	1.0898

Position	Radius(cm)	with Booster BII F(r,120)	with Booster BIII F(r,120)
A	139.70	1.000	1.0000
L	111.76	1.0466	1.0276
K	97.79	1.0495	1.0674
J	83.82	1.1039	1.0964
I	69.85	1.1330	–
H	55.88	1.2262	1.2423
G	41.91	1.2850	1.3373
F	27.94	1.4582	1.5018
E1	13.97	1.6265	1.6904
D	31.24	1.4148	1.4706
C	57.59	1.2087	1.2261
B	84.98	1.0935	1.1087

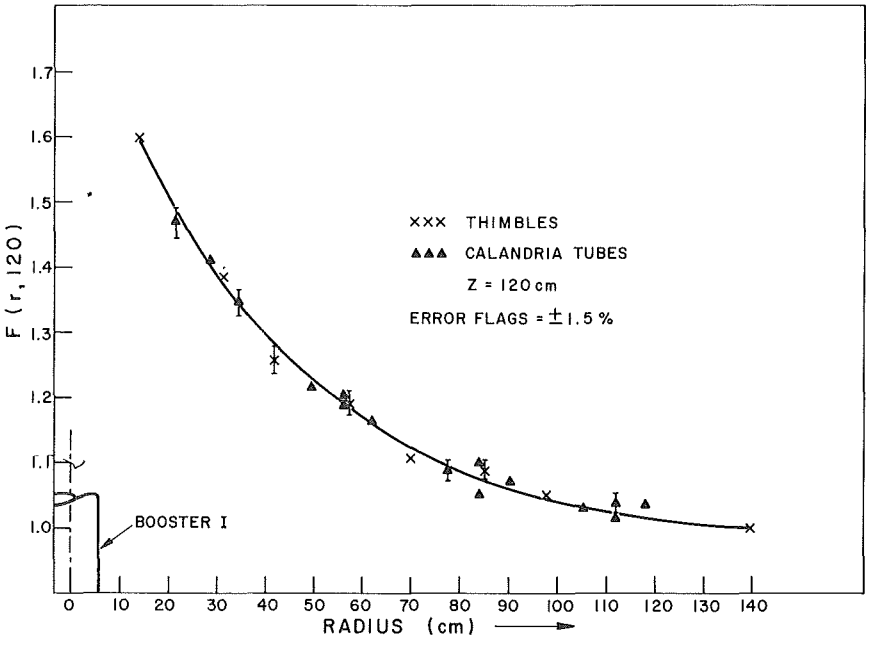

Fig. 16. Flux perturbation factor - rod-centred lattice with booster BI

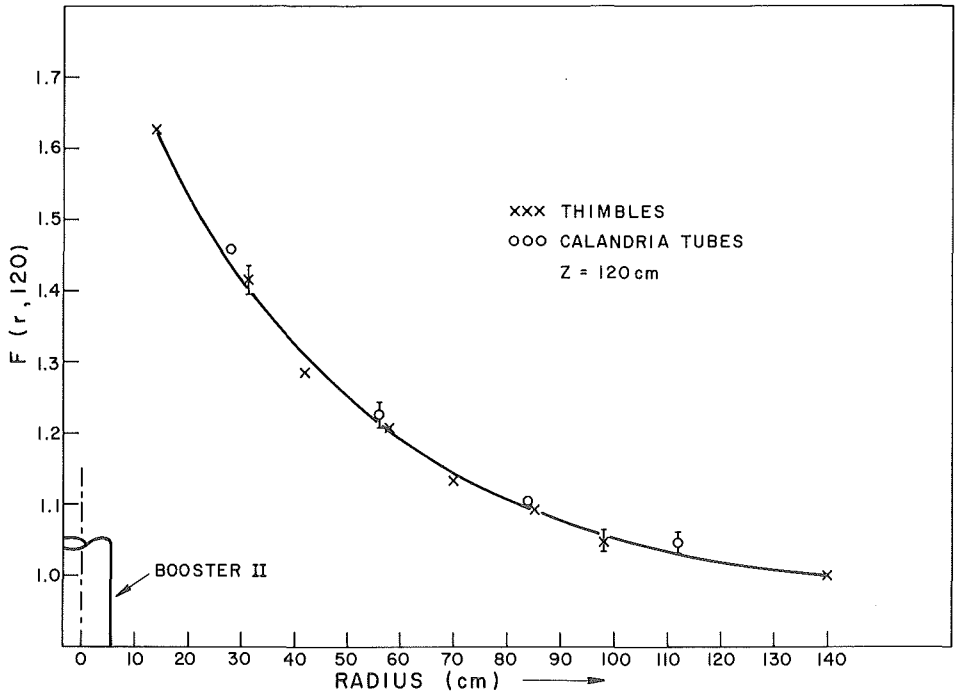

Fig. 17. Flux perturbation factor - rod-centred lattice with booster BII

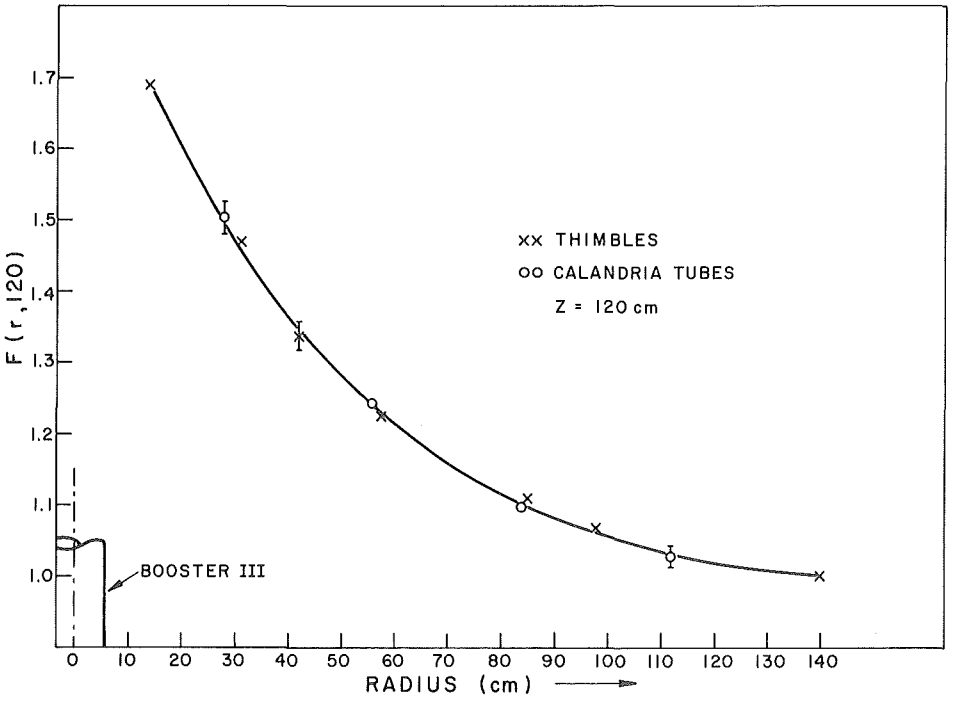

Fig. 18. Flux perturbation factor - rod-centred lattice with booster BIII

4.2 Fine Structure in the Booster Rods:

The neutron density distributions in the booster clusters were obtained from the measured activities at the surfaces of the fuel pin sheaths by correcting for the non-1/v epithermal activation through the use of the measured values of $r\sqrt{T_n/T_o}$.

The neutron densities in the clusters and at the surface of the support tube are listed in Tables 4 and 5 while the neutron densities in the surrounding moderator in two directions are given in Appendix II. The data are plotted in Fig. 19 - 24. From these figures it is seen that the neutron density depression in the clusters increases, as expected, with increasing U^{235} content. However the depression in the two zone 6.56 g/cm booster is larger than that for the 7.46 g/cm booster due to the loading of the U^{235} "high concentration" pins at the centre of the bundle. Moreover the neutron depression in the same booster is larger for the rod-centred lattice than for the open centre lattice.

The values of the average neutron density in the U-Al cores are not reported because the estimated errors are about ±5%, unusually high for this type of measurement. Two possible sources of errors are the variation in U^{235} concentration over the lengths of these cores (±4%) and the uneven gap widths between the two sections of each demountable element. Gap width differences of up to 0.25 mm were observed and may have caused small flux peaking in some gaps. These conditions could not be changed during the course of experiments, mainly due to the delay which would have resulted.

4.3 Reactivity Worths of the Boosters:

The reactivity worth of each booster was determined from the measurement of the change in critical height Δh when the booster was introduced into a reference lattice. The resulting changes in the axial buckling ΔB_z^2 were obtained using the expression:

$$\Delta B_z^2 = \pi^2 \left[\frac{1}{(h + \Delta h)^2} - \frac{1}{h^2} \right] \qquad (3)$$

Table 4. Fine structure in booster clusters - open centre lattice

Booster BI (5 g/cm)

Position	Normalized n.density z=105.1	Normalized n.density z=116.3	Average n.density in each zone
Surface of Support tube	1.7461	–	1.7461
R5	1.4014	1.3748	1.3876
	1.3738	1.3997	
R4	1.1964	1.2030	1.2027
	1.2012	1.2100	
R3	1.0795	1.0682	1.0812
	1.0866	1.0907	
R2	1.0158	–	1.0163
	1.0167	–	
R1	–	1.0000	1.0000

Booster BII (6.56 g/cm

Position	Normalized n.density z=116.3	Normalized n.density z=105.1	Average n.density in each zone
Surface of Support tube	2.1170	–	2.1170
R5	1.6261	1.6408	1.6451
	1.6587	1.6549	
R4	1.3868	1.4016	1.4068
	1.4513	1.3874	
R3	1.1422	1.1532	1.1529
	1.1536	1.1625	
R2	1.0515	1.0509	1.0516
	–	1.0523	
R1	0.9947	–	.9947

Booster BIII (7.46 g/cm)

Position	Normalized n.density z=105.1	Normalized n.density z=116.3	Average n.density in each zone
Surface of Support tube	2.0039	–	2.0039
R5	1.4908	1.4941	1.4908
	–	1.4874	
R4	1.2285	1.2290	1.2338
	–	1.2438	
R3	1.1041	1.1013	1.1001
	1.0950	1.1001	
R2	–	1.0231	1.0231
	–	–	
R1	–	–	–

Position	Radius, cm
Surface of Support tube	5.715
R5	4.427
R4	3.308
R3	2.215
R2	1.146
R1	0.000

Table 5. Fine structure in booster clusters - rod-centred lattice

Booster BI (5 g/cm)

Position	Normalized n.density z=105.1	Normalized n.density z=116.3	Average n.density in each zone
Surface of support tube	1.8083	–	1.8083
R5	1.4386	1.4568	1.4416
	1.4162	1.4547	
R4	1.2229	1.2217	1.2233
	1.2322	1.2164	
R3	1.0903	1.0893	1.0909
	1.0946	1.0892	
R2	1.0259	1.0237	1.0237
	1.0216	–	
R1	–	.9979	.9979

Booster BII (6.56 g/cm)

Position	Normalized n.density z=105.1	Normalized n.density z=116.3	Average n.density in each zone
Surface of Support tube	2.2480	–	2.2480
R5	1.7610	1.7693	1.7629
	1.7532	1.7682	
R4	1.4448	1.4746	1.4635
	1.4549	1.4796	
R3	1.1954	1.1742	1.1905
	1.1980	1.1945	
R2	1.0755	1.0726	1.0727
	1.0699	–	
R1	–	.9995	.9995

Booster BIII (7.46 g/cm)

Position	Normalized n.density z=105.1	Normalized n.density z=116.3	Average n.density in each zone
Surface of support tube	2.0650	–	2.0650
R5	1.5325	1.5657	1.5436
	–	1.5325	
R4	1.2560	1.2634	1.2591
	–	1.2578	
R3	–	1.1098	1.1124
	–	1.1149	
R2	1.0155	1.0155	1.0155
	–	–	
R1	–	1.0000	1.0000

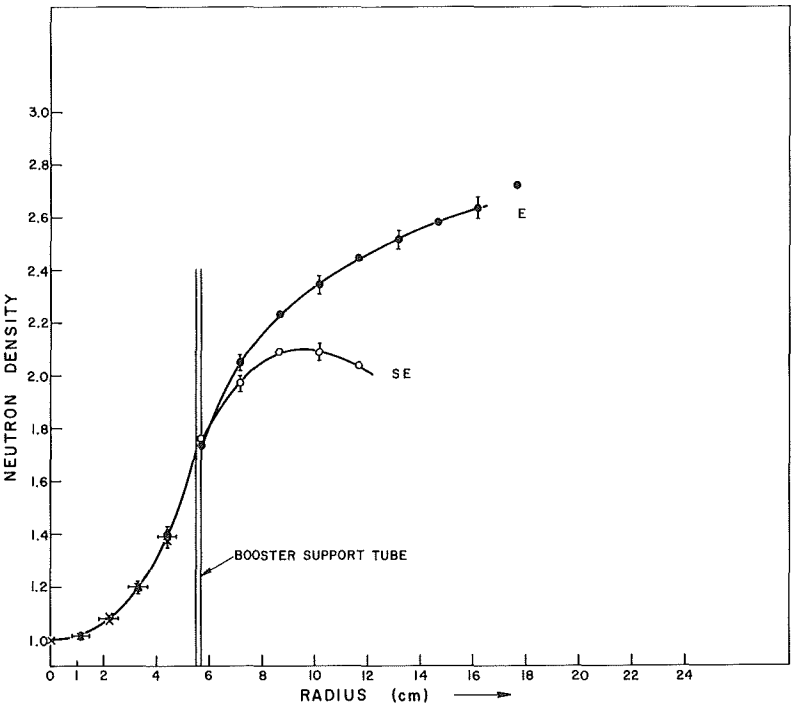

Fig. 19. Neutron density distribution in booster BI and moderator - open centre lattice

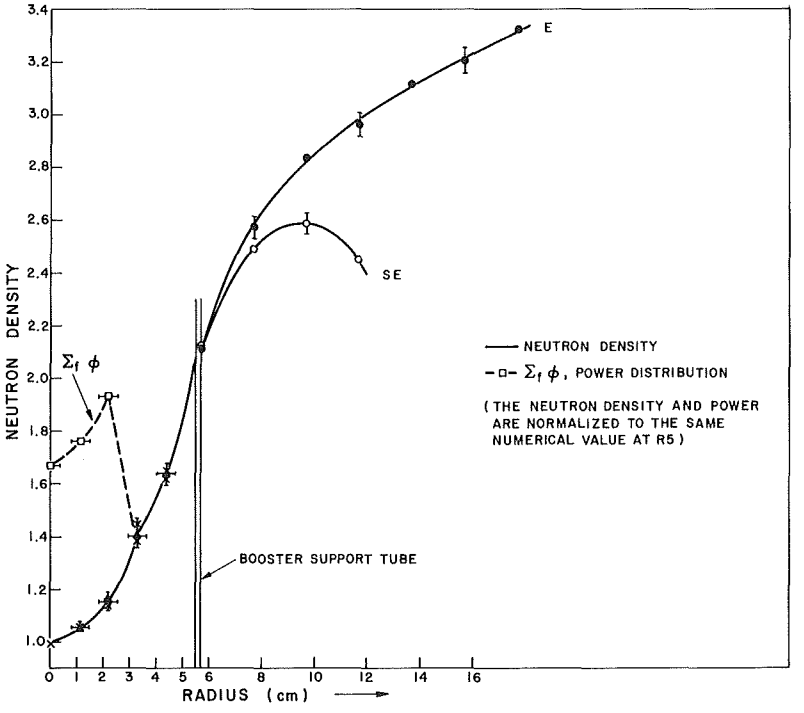

Fig. 20. Neutron density distribution in booster BII and moderator - open centre lattice

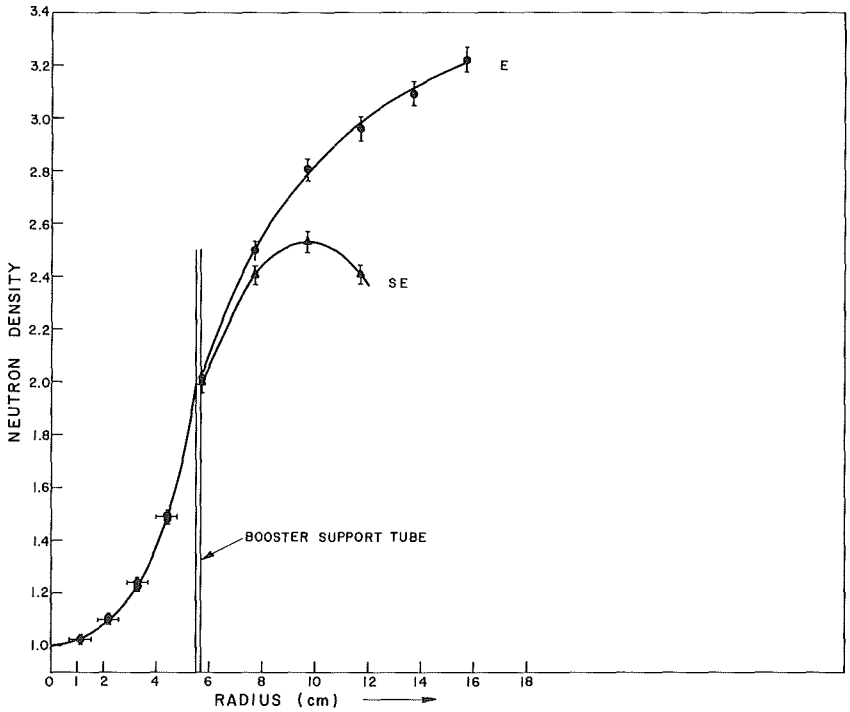

Fig. 21. Neutron density distribution in booster BIII and moderator - open centre lattice

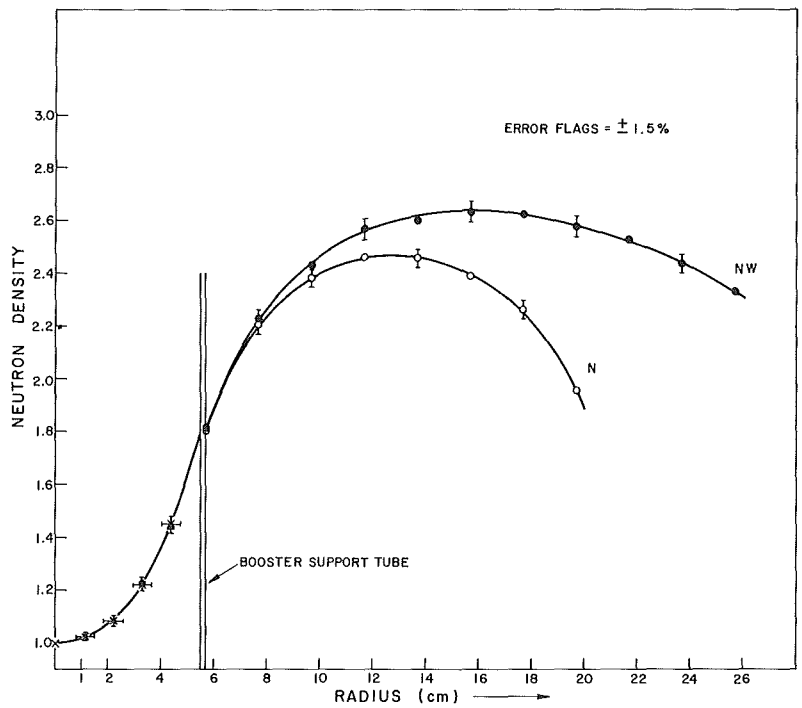

Fig. 22. Neutron density distribution in booster BI and moderator - Rod-centred lattice

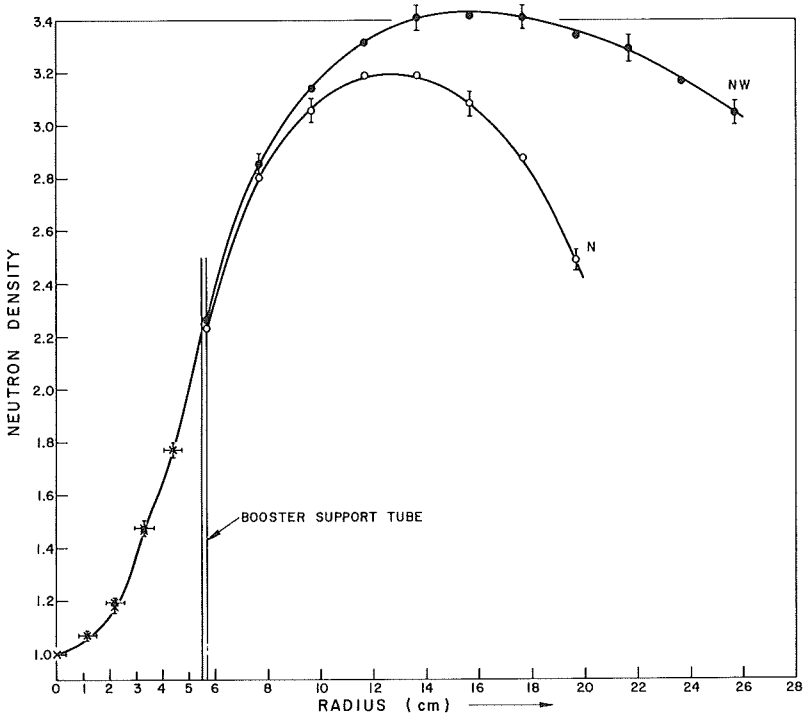

Fig. 23. Neutron density distribution in booster BII and moderator - rod-centred lattice

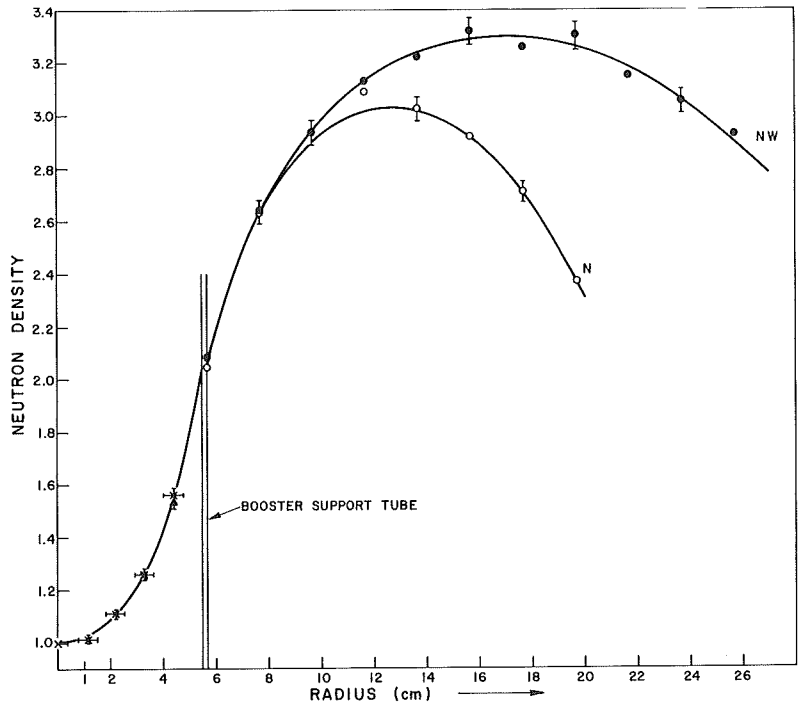

Fig. 24. Neutron density distribution in booster BIII and moderator - rod-centred lattice

where $h = (h_c + \delta'_z)$ is the extrapolated height of the unperturbed lattice and h_c is the unperturbed critical moderator level. The quantity δ'_z is related to the total axial extrapolation length δ_z by:

$$\delta'_z = \delta_z - 15 \qquad (4)$$

since the lower end of the fuel is 15 cm from the floor of the reactor vessel (see Fig. 7). δ_z was obtained from flux distribution measurements in the two reference lattices (Table 6).

Tables 7 and 8 give the critical heights, Δh and ΔB_z^2 for the different perturbations in the two lattices.

To convert the axial buckling changes into reactivity worths, use was made of the relation between δk and ΔB_z^2 obtained from two group diffusion theory, namely:

$$\delta k = F(h) \left[L^2 + L_s^2 + 2L^2 L_s^2 B^2 \right] \Delta B_z^2 \qquad (5)$$

where F(h) relates the change in radial buckling to the change of critical height of a particular lattice. L, L_s and B^2 are the thermal diffusion length, the slowing down length and the buckling respectively. B^2 was taken from measurements while L^2 and L_s^2 values were obtained from LATREP calculations (Table 9).

The only remaining undetermined term in Eq. (5) is F(h) which cannot be calculated easily. However it can be obtained from measurements with a Co wire whose reactivity effect can be calculated.

A full length Co wire inserted in a lattice at a position R_w from the centre of the lattice introduces a change in reactivity given by the following expression:

$$\delta k_{Co} = - \frac{(d\hat{\Sigma}_a V)_{Co} \; f \; (1 + L_s^2 B^2)}{(\hat{\Sigma}_a V)_{UO_2}} \cdot \frac{J_o^2 (\lambda R_w)}{N \left[J_o^2(\lambda R_c) + J_1^2(\lambda R_c) \right]} \qquad (6)$$

Table 6. Parameters of the reference lattice

	Open-centre Lattice	Rod-centred Lattice
Critical height, cm	200.32 ± 0.003	201.16 ± 0.003
Axial buckling, α^2, m^{-2}	1.975 ± 0.014	1.934 ± 0.014
Radial buckling, λ^2, m^{-2}	1.998 ± 0.020	2.101 ± 0.012
Extrapolated height, cm	223.57 ± 1.12	225.89 ± 1.14
Axial extrapolated length (δ)[(a)], cm	38.25	39.73
D_2O purity, atom%	99.72	99.72
Temperature, °C	21.2	21.3

(a) $\delta' = \delta - 15$

Table 7. Reactivity effects of the boosters - open centre lattice

Perturbation	Perturbed Critical height, cm	Δh, cm	ΔB_z^2, m^{-2}	Δk, mk	Temperature, °C
Booster BI at centre of pile	174.885	-25.635	+.5430	+25.34	21.01
Suspension system at centre of pile	201.554	+ 1.234	-.0216	- 1.01	21.23
Co-wire at Centre of pile	201.780	+ 1.460	-.0255	- 1.19	21.23
Booster BI at position G2E	176.163	-24.157	+.5074	+23.68	21.28
Suspension system at G2E	202.587	+ 1.186	-.0205	- 0.96	21.62
Booster BI at position G4E	179.853	-20.467	+.4181	+19.51	20.98
Suspension system at G4E	202.305	+ 0.904	-.0157	- 0.73	21.62
Booster BII at centre of pile	173.409	-27.913	+.5949	+27.76	21.41
Booster BIII at centre of pile	171.460	-29.941	+.6476	+30.22	21.93

$\delta' = 23.25$

Table 8. Reactivity effects of boosters - rod-centred lattice

Perturbation	Perturbed Critical height, cm	Δh, cm	ΔB_z^2, m^{-2}	Δk, mk	Temperature, ^0C
Booster BI at centre of pile	166.383	-34.710	+.7669	+32.64	21.15
Booster BI at position E4E	172.106	-29.049	+.6130	+26.09	21.47
Suspension system at centre of pile	207.032	+ 6.107	-.1009	- 4.29	21.40
Booster BII at centre of pile	163.682	-37.620	+.8485	+36.11	21.46
Booster BIII at centre of pile	160.774	-40.385	+.9339	+39.75	20.79
Co-wire at position E1E	202.634	+ 1.332	-.0225	- 0.96	21.46

$\delta' = 24.73$

Table 9. Parameters used in the calculations of the cobalt wire reactivity worth

Parameter		Open Centre lattice	Rod-centred lattice
B^2	m^{-2}	3.973	4.035
L^2	cm^2	223.30	223.30
L_S^2	cm^2	157.56	157.56
λ	m^{-1}	1.4135	1.4495
f	—	0.9343	0.9343
d	—	2.373	2.105
$\hat{\Sigma}_{UO_2}$	cm^{-1}	0.1780	0.1780
$\hat{\Sigma}_{CO}$	cm^{-1}	2.0857	2.091
V_{UO_2}	cm^3/cm	42.662	42.662
V_{CO}	cm^3/cm	0.0507	0.0507
N	—	52.	53.
R_C	cm	113.66	114.75
RW	cm	0.	13.97

where d is the flux advantage factor at the Co wire position, i.e. $\bar{\phi}_{Co}/\bar{\phi}_{UO_2}$ obtained from flux distribution measurement.

$\hat{\Sigma}_a$ is the effective absorption cross section,

V is the volume per unit length,

f is the thermal utilization,

N is the number of fuel assemblies in the lattice, and

R_c is the effective core radius and is given by

$$R_c = 27.94 \sqrt{N/\pi}$$

The values of the different parameters are given in Table 9. Using Eqs. (5) and (6) the following results are obtained:

δk_{Co} = -1.19 mk and F(h) = 1.142 for the open centre lattice, and

δk_{Co} = -0.957 mk and F(h)= 1.040 for the rod-centred lattice.

The values of the reactivity worths are now easily obtained for each ΔB_z^2 in Tables 7 and 8 assuming that F(h) is constant for each lattice for the range of critical heights measured in these experiments. These values are given in column 5 of these tables.

Errors in ΔB_z^2 due to temperature variations were deduced from LATREP calculations for the reference lattices at two different temperatures. By interpolation it was estimated that the temperature correction should be about 0.005 $m^{-2}/^{\circ}C$. Since the maximum variation in temperature during the measurements was less than 1°C (Tables 7 and 8), the corresponding uncertainty in ΔB_z^2 and hence in Δk is ~0.1% which is well within the experimental errors and thus could be neglected.

During the course of the experiments the D_2O purity varied from 99.752 wt % to 99.740 giving rise to an uncertainty in Δk of less than 0.2%.

Since ΔB_z^2 was determined from Eq. (3) and Δh was measured with an accuracy of ±0.003 cm the extrapolated critical height h must be the only serious source of error in ΔB_z^2. In fact h, obtained from least-squares fitting to experimental data, had an error of ±0.5%; thus the values of ΔB_z^2 are correct to within ±1.5%.

The uncertainty in the calculation of δk_{co} is essentially due to errors in d (~2%) assuming that the values of the effective cross-sections and volumes are correct. Errors in L_s^2 and B^2 may be neglected since the product $L_s^2 B^2$ is much less than unity. Thus δk_{co} is accurate to ±2% and the uncertainty in F(h) is ±2.5%.

From these errors the uncertainty in the measured values of Δk given in Tables 7 and 8 is estimated to be ±3%.

The reactivities of the boosters are plotted in Fig. 25 as a function of U^{235} concentration per unit length. It is evident that the reactivity is not proportional to the U^{235} concentration. This may be attributed to the self-shielding in these strongly absorbing boosters. The geometry of the two-zone 6.56 g/cm booster introduces a further decrease in reactivity since the high concentration elements at the central region are shielded by the low concentration elements; the more reactive elements are in the region of least importance. This arrangement, however, has the practical advantage of improving the heat transfer in the booster because of the power flattening obtained (see Fig. 20).

It is also noted that the reactivity values for the open centre lattice are much lower than those for the rod centred lattice. This is because locating a booster in an interstitial position increases the fuel to moderator ratio in the surrounding area, thus resulting in larger mutual shielding which reduces the effectiveness of the booster. For example - the reactivity gain resulting from moving the 5 g/cm booster from the interstitial position to the position of a central fuel assembly is about 29%. In contrast, replacing this booster in the interstitial position by the 7.46 g/cm booster (i.e. an increase of 49% in U^{235}) results in only a 19% increase in reactivity.

The reactivity of the 5 g/cm booster is shown in Fig. 26 for different radial positions. It can be seen that near the centre of the reactor the reactivity change is essentially proportional to the square of the flux. However at a distance of about two lattice pitches from the centre the disagreement between measurement

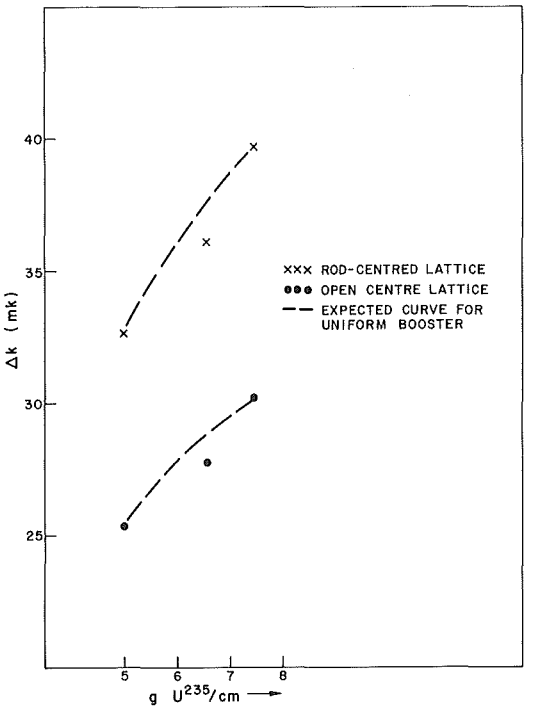

Fig. 25. Reactivity effects of the boosters

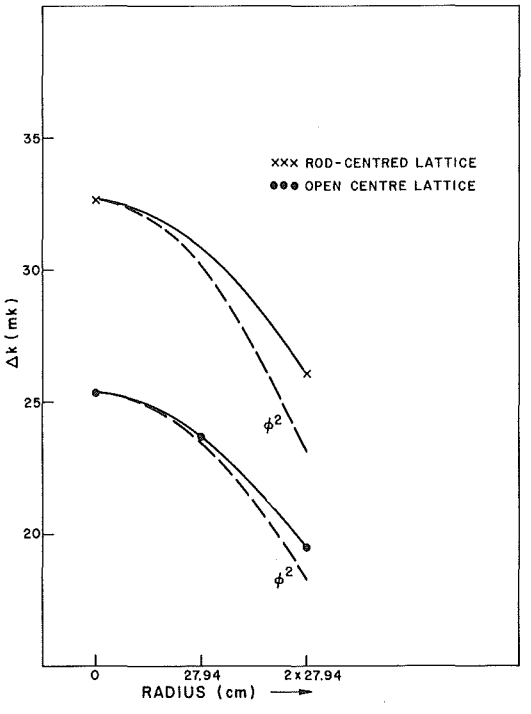

Fig. 26. Reactivity effects of booster BI at different radial positions

and ϕ^2 increases due to the fact that for such a large perturbation the reactivity is proportional to the product of the unperturbed and the perturbed fluxes.

5. CONCLUSIONS

Measurements were performed in ZED-2 on simulated BLW boosters containing different concentrations of U^{235} per unit length. These boosters either replaced the central fuel assembly in a rod-centred lattice or were located interstitially in an open centre lattice.

Each booster acting as a strong source of fast neutrons and a sink for thermal neutrons resulted in an appreciable flux perturbation in the host lattice and in a large peak in the vicinity of the booster. This peaking, however, was less in the open centre lattice than in the rod-centred lattice due to the larger mutual shielding resulting from higher fuel to moderator ratio in the region of the booster. This also explains the results of reactivity measurements which showed that the boosters were more reactive when they replaced a fuel assembly in the core than when they were suspended interstitially in a vertical position.

Moreover, it was found that neither the flux peaking in the lattices nor the reactivity effect was proportional to the U^{235} concentration in the boosters due to self-shielding.

ACKNOWLEDGEMENTS

The author is very grateful to E. Critoph for his helpful comments and assistance in the presentation of this report, to P. French for reading and commenting on the original manuscript, to Dr. R.E. Green for his helpful advice during the course of the experiment, and to Dr. A. Okazaki for numerous interesting discussions.

The author also thanks P.D.J. Ferrigan, E. Pleau and D.J. Roberts for their help in performing the measurements, D.A. Kettner for foil counting, Miss D. McKee for running the data reduction programs and Mrs. N. Hulbert for typing the manuscript.

REFERENCES

1. R.E. Kay; CANDU-BLW Experiments in ZED-2, Part II: Booster Rod Experiments. AECL-2689 (1967)

2. R.E. Kerr; private communication

3. B.M. Townes; private communication

4. D.H. Walker; private communication.

APPENDIX I

Radial and Axial Flux Distributions

Table I-1

Normalized Activities in the Open Center Reference Lattice

(See Figure 8)

Elevation (cm)	F9	F7	F6	F5	F4	F3	F2	F1	F0	G	E	D	C	B
200	.0731													
190	.2394		.2962					.2888	.4265	.4764				
180	.3807		.4815					.4756	.7012	.7944				
170	.5136		.6458					.6493	.9550	1.0817				
160	.6277		.8079					.8086	1.1844	1.3448				
150	.7347		.9351					.9274	1.3857	1.5668				
140	.8200		1.0431					1.0410	1.5591	1.7693				
130	.8909		1.1421					1.1389	1.6940	1.9279				
120	.9471	.7173[N]	1.2276	.9451[N]	1.5274	1.1398[N]	1.7252	1.2236	1.8153	2.0544	1.6872	1.4104	1.0533	.9739
S		.6954		.9283		1.1035		1.2027						
E		.6735		.8831		1.0764		1.2264						
W		.7564		.9907		1.1300		1.1957						
110	-		1.2884					1.2917	1.8933	2.1590				
100	-		1.2919					1.2851	1.9259	2.2014				
90	1.0000	.7546[N]	1.2963	.9959[N]	1.6163	1.1868[N]	1.8284	1.2851	1.9259	2.2034	1.7782	1.4914	1.1150	1.0356
S		.7210		.9660		1.1561		1.2581						
E		.6964		.9195		1.1417		1.2735						
W		.7877		1.0317		1.1934		1.2581						
80	-		1.2728					1.2586	1.8963	2.1623				
70	-		1.2325					1.2227	1.8311	2.0749				
60	.8918		1.1628					1.1789	1.7293	1.9607				
50	.8174		1.0512					1.0448	1.5780	1.7869				
40	.7254		.9352					.9246	1.3982	1.5893				
30	.6215		.8070					.8095	1.2171	1.3833				
20	.5025		.6972					.7411	1.0645	1.1881				
10			.6032					-	.9346	.9876				

[N]North position on calandria tube

Table I-2

Normalized Activities in the Open Center Lattice Containing

Booster BI (5 g/cm) - See Figure 10

Elevation (cm)	F9	F7	F6	F5	F4	F3	F2	F1	F0	E	D	C	B
170	.1761		.2278					.2572	.3533				
160	.3494		.4623					.5140	.7434				
150	.5037		.6638					.7394	1.0869				
140	.6350		.8429					.9565	1.3968				
130	.7465		1.0003					1.1360	1.6681				
120	.8353	.6589[N]	1.1460	.9039[N]	1.5085	1.1829[N]	1.8876	1.3049	1.8769	1.7501	1.3524	.9639	.8561
S		.6248		.8865		1.1407		1.3288					
E		.6067		.8228		1.0933		1.3342					
W		.6883		.9489		1.1878		1.2509					
110	.9914		1.2566					1.4532	2.0949				
100	.9274		1.3135					1.5067	2.1962				
90	(1.0000)*	.7742[N]	1.3539	1.0663[N]	1.8052	1.3790[N]	2.2725	1.5472	2.2565	2.1016	1.6093	1.1439	1.0214
S		.7342		1.0412		1.3314		1.5589					
E		.7158		.9694		1.2855		1.5667					
W		.8133		1.1333		1.4261		1.5013					
80	.9519		1.3671					1.5545	2.2798				
70	1.0073		1.3533					1.5525	2.2385				
60	.9920		1.2930					1.4979	2.1482				
50	.8815		1.1904					1.3647	1.9813				
40	.7869		1.0695					1.2166	1.7798				
30	.6797		.9387					1.0639	1.5637				
20	.5493		.8157					.9952	1.3870				
10	-		.7054					-	1.2593				

*Value obtained from least squares fitting to Cos $\alpha(Z-Z_o)$.

[N]North position on calandria tube

Table I-3

Normalized Activities in the Open Center Lattice Containing Booster BII (6.56 g/cm) - See Figure 10

Elevation (cm)	F9	F7	F6	F5	F4	F3	F2	F1	F0	E	D	C	B
170	.1425		.1834						.2857				
160	.3235		.4256						.7015				
150	.4810		.6330						1.0576				
140	.6162		.8147						1.3749				
130	.7202		.9875						1.6614				
120	.8339	.6438[N]	1.1315	.9044[N]	1.4961	1.1595[N]	1.8884	1.3220[N]	1.8849	1.7807	1.3338	.9521	.8455
S		.6295		.8712		1.1442		1.3442					
E		.5972		.8144		1.0916		1.3630					
W		.6868		.9591		1.2103		1.2673					
110	.9091		1.2466						2.1150				
100	.9657		1.3091						2.2310				
90	1.0000	.7636[N]	1.3580	1.0839[N]	1.8206	1.4073[N]	2.3110	1.5709[N]	2.3093	2.1141	1.6011	1.1465	1.0084
S		.7507		1.0381		1.3474		1.5857					
E		.7139		.9772		1.3057		1.5970					
W		.8127		1.1244		1.4599		1.5457					
80	1.0097		1.3684						2.3162				
70	.9911		1.3542						2.3171				
60	.9485		1.2932						2.2156				
50	.8852		1.2021						2.0362				
40	.8001		1.0860						1.8402				
30	.6876		.9569						1.6125				
20	.5664		.8329						1.4369				
10	-		.7249						1.3016				

[N] North position on calandria tube

Table I-4

Normalized Activities in the Open Center Lattice Containing

Booster B III (7.46 g/cm) - See Figure 10

Elevation (cm)	F9	F7	F6	F5	F4	F3	F2	F1	F0	E	D	C	B
170	.1050		.1317						.1985				
160	.2963		.3866						.6446				
150	.4552		.6054						1.0185				
140	.5964		.7964						1.3655				
130	.7022		.9755						1.6614				
120	.8206	.6453[N]	1.0861	.8987[N]	1.5224	1.1649[N]	1.8987	1.3374[N]	1.8873	1.7996	1.3441	.9453	.8372
S		.6164		.8778		1.1534		1.3249					
E		.5948		.8187		1.0986		1.3892					
W		.6812		.9576		1.2276		1.2864					
110	.8966		1.2447						2.1433				
100	.9599		1.3284						2.2882				
90	1.0000	.7752[N]	1.3710	1.0845[N]	1.8502	1.4253[N]	2.3476	1.6181[N]	2.3546	2.1558	1.6352	1.1497	1.0248
S		.7530		1.0575		1.3869		1.6306					
E		.7176		.9861		1.3259		1.6457					
W		.8229		1.1446		1.4889		1.5895					
80	1.0115		1.3819						2.3902				
70	.9955		1.3699						2.3690				
60	.9552		1.3198						2.2807				
50	.8908		1.2222						2.0998				
40	.7955		1.1008						1.8902				
30	.6939		.9652						1.6606				
20	.5614		.8483						1.4742				
10	-		.7387						1.3359				

[N] North position on calandria tube

Table I-5

Normalized Activities in the Rod-Centered Reference Lattice

(See Figure 9)

Elevation (cm)	A	L	K	J	I	H	G	F-S	E0	E1	D	C	B
190	.2558				.4645			.4014		.5715			
180	.3959				.7542			.6496		.9311			
170	.5223				1.0219			.8894		1.3212			
160	.6377				1.2640			1.1016		1.6132			
150	.7346				1.4598			1.2607		1.8844			
140	.8215				1.6411			1.4098		2.1154			
130	-				1.7897			1.5495		2.3274			
120	(.9492)*	.7694[N]	1.4514	1.0520[N]	1.9168	1.3800[N]	2.3049	1.6092	1.7011[N]	2.4989	2.3984	2.1088	1.6598
S		.8920		1.2044		1.4934		1.6660	1.6702				
E		.8503		1.1109		1.4332		1.6026	1.6868				
W		.8282		1.1551		1.4246		1.6656	1.6775				
110	.9914				2.0138			1.7480		2.6108			
100	-				2.0397			1.7458		2.6314			
90	1.0000	.7952[N]	1.5300	1.1122[N]	2.0308	1.4313[N]	2.4420	1.6807	1.7757[N]	2.6372	(2.5620)*	2.2286	1.7549
S		.9375		1.2529		1.5475		1.7435	1.7650				
E		.8883		1.1522		1.4937		1.6894	1.7733				
W		.8594		1.2098		1.4844		1.7071	1.7598				
80	-				1.9984			1.7066		2.5878			
70	-				1.9193			1.6603		2.5140			
60	-				1.8107			1.5971		2.3805			
50	.8182				1.6710			1.4253		2.1886			
40	.7316				1.4838			1.2660		1.9498			
30	.6313				1.2964			1.1101		1.7129			
20	.5262				1.1215			1.0077		1.5020			
10	.4047				.9726			-		1.3145			

*Value obtained from least squares fitting to Cos α $(Z-Z_o)$

[N]North position on calandria tube

Table I-6

Normalized Activities in the Rod-Centered Lattice Containing

Booster B I (5 g/cm) - See Figure 11

Elevation (cm)	A	L	K	J	I	H	G	F-S	El	D	C	B
190	.0724				.0800			.0944	.1037			
180	.0762				.0923			.1147	.1250			
170	.0802				.1100			.1510	.1574			
160	.2324				.4473			.5060	.7372			
150	.4133				.8512			.9633	1.5259			
140	.5621				1.2030			1.3726	2.2272			
130	.6926				1.5262			1.7457	2.8473			
120	.7904	.6628[N]	1.2698	.9374[N]	1.7712	1.3364[N]	2.4167	1.8075	3.3266	2.7644	2.0950	1.5063
S		.7648		1.0925		1.5112		2.0377				
E		.7192		1.0157		1.4179		1.8836				
W		.7161		1.0097		1.4278		1.9527				
110	.8932				2.0324			2.3484	3.8106			
100	.9620				2.1948			2.5020	4.1223			
90	1.0000	.8080[N]	1.6050	1.1777[N]	2.2835	1.6588[N]	3.0816		4.3387	3.4613	2.6141	1.8801
S		.9666		1.3903		1.9013		2.6005				
E		.8990		1.2656		1.7791						
W		.8963		1.2972		1.7793						
80	1.0194				2.3137			2.6717	4.4192			
70	1.0094				2.3183			2.6640	4.4067			
60	.9753				2.2605			2.5958	4.2431			
50	.9124				2.0928			2.3596	3.9742			
40	.8278				1.8966			2.1317	3.5784			
30	.7267				1.6665			1.8625	3.1556			
20	.6064				1.4716			1.6725	2.6899			
10	.4696				1.2945			-	2.2869			

[N]North position on calandria tube

Table I-7

Normalized Activities in the Rod-Centered Lattice Containing Booster B II (6.56 g/cm) - See Figure 11

Elevation (cm)	A	L	K	J	I	H	G	F	El	D	C	B
160	.1808				.3297				.5259			
150	.3708				.7670				1.3821			
140	.5334				1.1457				2.1238			
130	.6734				1.4835				2.7934			
120	.7743	.6561[N]	1.2425	.9368[N]	1.7715	1.3447[N]	2.4161	1.8319[N]	3.3156	2.7681	2.0793	1.4806
S		.7581		1.0955		1.5360		2.0857				
E		.7196		1.0297		1.4292		1.8852				
W		.7173		1.0106		1.4259		1.9981				
110	.8843				2.0415				3.8587			
100	.9515				2.1857				4.1411			
90	1.0000	.8219[N]	1.5890	1.2001[N]	2.3107	1.7146[N]	3.1767	2.4649[N]	4.3864	3.5850	2.6613	1.9040
S		.9814		1.4133		1.9759		2.5354				
E		.9161		1.3088		1.8202		2.7154				
W		.9061		1.3098		1.8120		2.3422				
80	1.0229				2.3658				4.5394			
70	1.0069				2.3599				4.5438			
60	.9660				2.3122				4.3881			
50	.9232				2.1461				4.0871			
40	.8378				1.9420				3.6993			
30	.7300				1.7175				3.2220			
20	.6214				1.5108				2.7606			
10	.4788				1.3330				2.3647			

[N] North position on calandria tube

Table I-8

Normalized Activities in the Rod-Centered Lattice Containing Booster B III (7.46 g/cm) - See Figure 11

Elevation (cm)	A	L	K	J	I	H	G	F	El	D	C	B
160	.1213				.6694				.2676			
150	.3324				1.0810				1.2215			
140	.5016				1.4368				2.0393			
130	.6417				1.7536				2.7766			
120	.7536	.6251[N]	1.2299	.8950[N]	2.0327	1.3131[N]	2.4471	1.8251[N]	3.3534	2.8001	2.0527	1.4609
S		.7262		1.0684		1.5264		2.0934				
E		.6810		.9998		1.4380		1.9133				
W		.6924		.9747		1.3792		1.9729				
110	.8649				2.2105				3.9326			
100	.9453				2.3234				4.2484			
90	1.0000	.8086[N]	1.6161	1.1866[N]	2.4082	1.8396[N]	3.2678	2.4229[N]	4.5312	3.7277	2.7205	1.9392
S		.9760		1.4190		1.9756		2.8129				
E		.9181		1.3362		1.9148		2.5625				
W		.9230		1.2835		1.8091		2.6348				
80	1.0228				2.4116				4.7564			
70	1.0212				2.3592				4.7494			
60	.9799				2.1937				4.5541			
50	.9308				2.0082				4.3230			
40	.8528				1.7829				3.8608			
30	.7408				1.5637				3.4019			
20	.6171				1.3859				2.8801			
10	.4757				-				2.5040			

[N] North position on calandria tube

APPENDIX II

Activity Distribution in the D_2O Moderator Surrounding the boosters

Open Centre Lattice

Booster BI (5 g/cm)

Activity Distribution

Radius (cm)	E direction	SE direction
5.71[a]	1.7329	1.7594
7.21	2.0516	1.9695
8.71	2.2338	2.0909
10.21	2.3450	2.0885
11.71	2.4446	2.0374
13.21	2.5157	
14.71	2.5862	
16.21	2.6369	
17.71	2.7235	

Booster BII (6.56 g/cm

Activity Distribution

Radius (cm)	E direction	SE direction
5.71[a]	2.1157	2.1183
7.71	2.5758	2.4878
9.71	2.8333	2.5892
11.71	2.9662	2.4526
13.71	3.1173	
15.71	3.2103	
17.71	3.3266	

Booster BIII (7.46 g/cm)

Activity Distribution

Radius (cm)	E direction	SE direction
5.71[a]	2.0130	1.9948
7.71	2.4997	2.4047
9.71	2.8072	2.5306
11.71	2.9613	2.4101
13.71	3.0950	
15.71	3.2235	

a) Surface of the support tube.

Rod-Centred Lattice

Booster I (5 g/cm)

	Activity Distribution	
Radius (cm)	NW direction	N direction
5.71[a]	1.8060	1.8106
7.71	2.2297	2.2056
9.71	2.4324	2.3860
11.71	2.5693	2.4628
13.71	2.6000	2.4569
15.71	2.6339	2.3936
17.71	2.6275	2.2652
19.71	2.5797	1.9589
21.71	2.5277	
23.71	2.4418	
25.71	2.3349	

Booster II (6.56 g/cm)

	Activity Distribution	
Radius (cm)	NW direction	N direction
5.71[a]	2.2638	2.2323
7.71	2.8543	2.8067
9.71	3.1394	3.0609
11.71	3.3138	3.1921
13.71	3.4113	3.1879
15.71	3.4186	3.0850
17.71	3.4101	2.8777
19.71	3.3434	2.4869
21.71	3.2893	
23.71	3.1694	
25.71	3.0463	

Booster III (7.46 g/cm)

	Activity Distribution	
Radius (cm)	NW direction	N direction
5.71[a]	2.0849	2.0450
7.71	2.6391	2.6353
9.71	2.9385	–
11.71	3.1304	3.0928
13.71	3.2258	3.0250
15.71	3.3203	2.9193
17.71	3.2606	2.7087
19.71	3.3071	2.3713
21.71	3.1483	
23.71	3.0500	
25.71	2.9266	

a) Surface of the support tube.